Advances in Production Engineering & Management
Volume 21 | Number 2 | June 2026 | pp 268–275
https://doi.org/10.14743/apem2026.2.573
ISSN 1854-6250
Journal home: apem-journal.org
Original scientific paper

Premature failure analysis of a high-strength hot-dip galvanized 42CrMo4 steel bolt

Bulatović, S.[a,*], **Kovačević, Z.**[a], **Aleksić, V.**[a], **Samardžić, I.**[b]

[a]Institute for Materials Testing (IMS), Belgrade, Serbia
[b]Mechanical Engineering Faculty, University of Slavonski Brod, Slavonski Brod, Croatia

A B S T R A C T

This study investigates the premature failure of a high-strength hot-dip galvanized 42CrMo4 steel bolt of property class 10.9 used in a spatial steel structure. The aim was to identify the most likely failure mechanism and provide a basis for preventing similar failures. The investigation included visual and macrographic examination, optical emission spectroscopy, light optical microscopy (LOM), zinc-coating thickness evaluation, and Vickers hardness testing (HV1). The fracture occurred at the head-to-shank junction. The steel exhibited a tempered martensitic microstructure with banding, while the zinc coating was 82-155 µm thick and showed local damage and cracking. Hardness values ranged from 330 to 401 HV1, with several measurements exceeding 350 HV1. All measured alloying elements except carbon were within the nominal composition ranges for 42CrMo4 steel. Considering the fracture morphology, elevated local hardness, coating condition, and short time to failure, hydrogen embrittlement was identified as the most likely failure mechanism. These findings illustrate the value of combining fracture-surface observations, metallography, coating assessment, and hardness measurements in the failure analysis of high-strength galvanized fasteners. From a practical perspective, the results may support more informed selection, inspection, and quality control of high-strength fasteners, thereby helping to reduce the risk of similar premature failures.

A R T I C L E I N F O

Keywords:
Failure analysis;
High-strength bolt;
Hydrogen embrittlement;
Hot-dip galvanizing;
42CrMo4 steel;
Head-to-shank junction;
Optical microscopy;
Vickers hardness

**Corresponding author:*
srdjan.bulatovic@institutims.rs
(Bulatović, S.)

Article history:
Received 11 June 2026
Revised 29 June 2026
Accepted 5 July 2026

1. Introduction

This paper analyses the fracture of a high-strength class 10.9 bolt used in the steel structure of Hall 3 of the historic fair complex. The bolt failed just a few days after installation and before the facility was put into use. The bolt was hot-dip galvanized for better corrosion resistance. Numerous studies have analysed premature failures of high-strength hot-dip galvanized bolts in service.

In a broader production-engineering context, quality control in steel production increasingly combines conventional inspection techniques with data-driven methods, including machine learning, to identify defects and relate them to manufacturing-process conditions [1, 2]. Boyd and Hyler [3] highlighted the susceptibility of galvanized high-strength bolts to hydrogen-stress cracking and stress-corrosion cracking. Townsend [4] likewise showed that zinc coatings can reduce the fracture resistance of high-strength AISI 4140 steel (approximately equivalent to 42CrMo4) and that susceptibility depends strongly on material hardness. These findings underline the importance of controlling hardness, hydrogen sources, and galvanizing conditions in high-strength fasteners. Other authors [5-10] have investigated the micromechanisms of crack initiation and propagation, including liquid metal embrittlement (e.g., molten zinc on steel), hydrogen-induced cracking, and quench cracking.

Liquid metal embrittlement occurs when a normally ductile solid metal comes into contact with a liquid metal of lower melting point (e.g., molten zinc on steel). Under the action of tensile stress, the liquid atoms penetrate the grain boundaries of the solid material, severely weakening the cohesion and causing sudden intercrystalline cracks.

Hydrogen-induced cracking (HIC), often referred to as hydrogen embrittlement, occurs when atomic hydrogen enters and diffuses through the metal lattice, as illustrated in Fig. 1 [11]. The accumulated hydrogen reduces ductility and causes localised embrittlement. Under residual or applied stresses, the metal experiences cracking, predominantly intercrystalline or along inclusion boundaries.

Quench cracking is caused by high thermal and transformation stresses generated during rapid cooling (quenching) in heat-treatment processes. If the material is too brittle or has high carbon content, these stresses exceed the material's strength, forming cracks.

The analysis of the bolt in question should therefore consider the applicable standards [12-16] governing high-strength structural bolting, steel designation and composition, hot-dip galvanized coatings, and Vickers hardness testing.

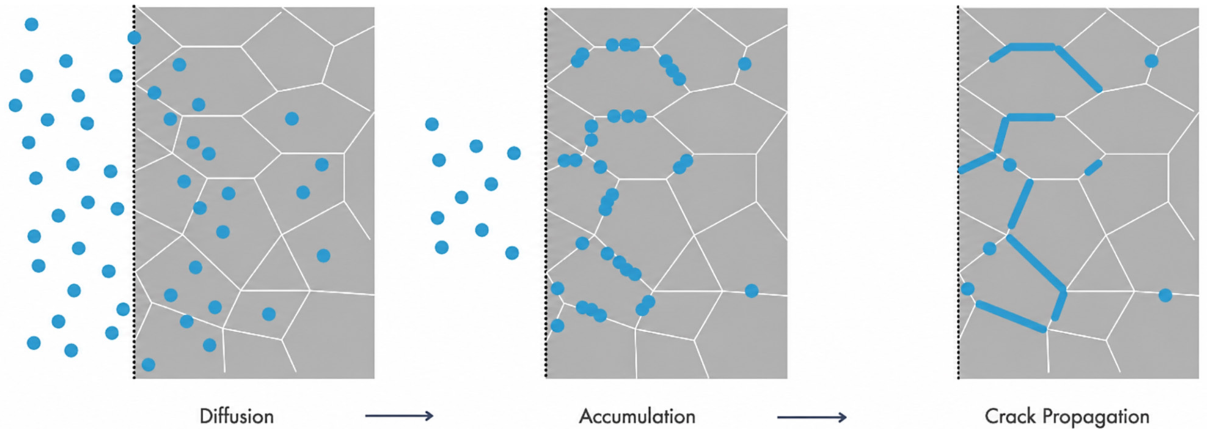

Fig. 1 Hydrogen embrittlement mechanism (adapted from [11])

2. Materials and methods

2.1 Description of the bolt

A bolt that failed a few days after installation was taken to the laboratory to determine the possible cause of the failure. The bolt had a hexagonal head, an M27 metric thread, a nominal length of 105 mm, and property class 10.9, in accordance with EN 14399-4 [12]. The steel designation 42CrMo4 follows EN 10027-1 [13], and its nominal chemical composition according to EN 10083-3 [14] is shown in Table 1.

According to the technological process specified in the technical documentation, the bolt is hot forged, hardened and tempered. After heat treatment, it is hot-dip galvanized. A tempered martensitic microstructure was therefore expected.

The broken bolt that was received for testing is shown in Fig. 2.

Table 1 Nominal chemical composition of 42CrMo4 steel (wt.%)

C	Si	Mn	P	S	Cr	Mo
0.38-0.45	max. 0.4	0.6-0.9	max. 0.025	max. 0.035	0.9-1.2	0.15-0.3

Fig. 2 Broken bolt that was received for testing

2.2 Experimental procedure

The high-strength hot-dip galvanized 42CrMo4 steel bolt investigated in this study experienced a premature brittle fracture at the critical head-to-shank junction. To determine the underlying cause of the fracture and characterise the material, the investigation included the following stages:

Visual inspection and macrographic analysis: Macroscopic evaluation of the fractured bolt to identify surface anomalies, fracture morphology, and the overall crack path.

Determination of chemical composition: Quantitative chemical analysis to verify nominal steel grade compliance and identify potential localised compositional deviations.

Microstructure examination: Optical characterisation of the steel microstructure and the condition of the zinc coating.

Microhardness measurements: Measurements in the subsurface fracture zone to assess local hardness variations relevant to embrittlement.

3. Test results

3.1 Visual inspection and macrographic analysis

The initial phase of the failure analysis involved non-destructive macrostructural screening of the fractured bolt component. Visual inspection and macro-photography were performed using an optical microscope equipped with a high-resolution digital image capture system. This stage focused on mapping the exact crack initiation site, evaluating the spatial propagation path across the fracture cross-section, and identifying the macrographic topography. Special attention was directed to the geometric transition zone at the head-to-shank fillet junction to evaluate mechanical tolerances, assembly alignments, and the physical integrity of the protective hot-dip galvanized coating layer directly adjacent to the main fracture path.

Fig. 3 shows the fracture surface of the bolt on both the head and shank. A cross-section of bolt failure shows two clearly distinct areas: a smooth area along the entire outer edge and a quasi-circular rough region located in the central part of the cross-section of the bolt. The rough, central region of the failure surface has a significantly smaller area compared to the zone of stable crack propagation. The failure is straight, perpendicular to the axis of the bolt, see also Fig. 2.

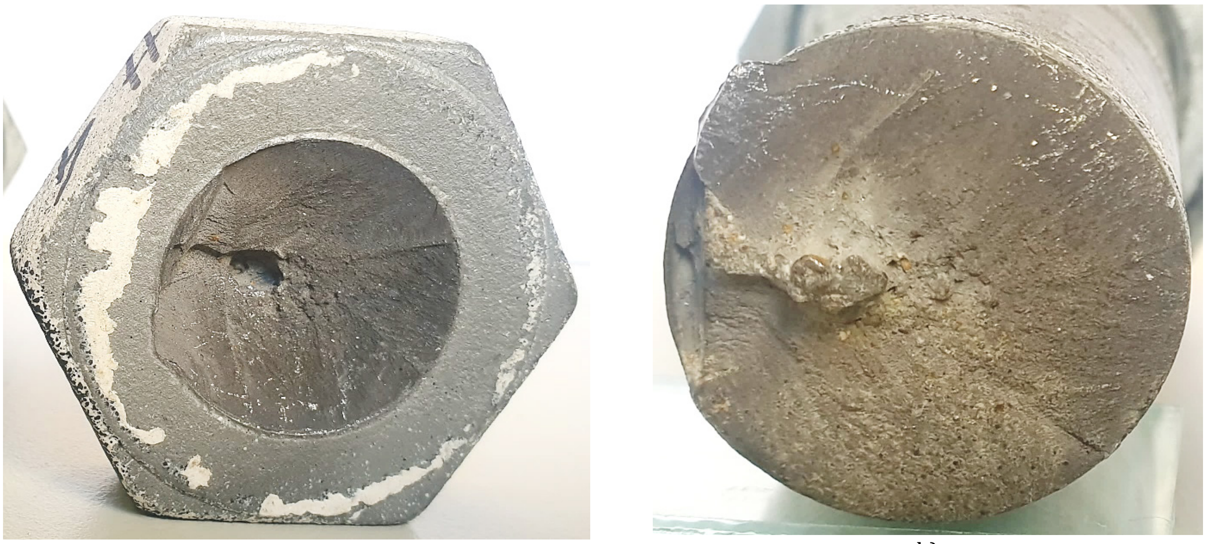

a) b)

Fig. 3 Fracture surfaces on the received bolt: (a) head; (b) shank

3.2 Chemical composition

Chemical analysis was carried out using optical emission spectroscopy, and the results are shown in Table 2. Compared with the nominal ranges in Table 1, all measured elements except carbon are within the specified composition limits for 42CrMo4 steel.

The chemical analysis indicates that the carbon content (0.339 wt.%) is below the nominal standard range for 42CrMo4 steel (0.38-0.45 wt.%). This deviation may result from minor surface decarburization during heat treatment or from local chemical heterogeneity. Although the lower carbon content could marginally reduce the peak attainable hardness, the material still exhibited a hardened tempered martensitic microstructure, as discussed below.

Table 2 Measured chemical composition of 42CrMo4 steel (wt.%)

C	Si	Mn	P	S	Cr	Mo
0.339	0.21	0.78	0.012	0.011	0.98	0.16

3.3 Microstructural analysis

Fig. 4 shows a sectioned part of the bolt shank with the fracture surface and the mounted metallographic samples marked 1 and 2. The preparation procedure for samples 1 and 2 included grinding, mechanical polishing, and etching with 3 % nital.

Grinding removed the deep marks left by the cutting and created a flat surface. The process was carried out gradually, using wet sandpaper of increasing grit, from coarse to fine.

Mechanical polishing was performed on rotating discs with the addition of aluminium oxide until a high-gloss surface was obtained. Diamond paste was used for final polishing.

Etching with 3 % nital (a mixture of 3 % nitric acid and ethanol) selectively revealed the microstructure for optical microscopy.

Mounted samples were used for both microstructure analysis and microhardness analysis.

Metallographic analysis of the cross-section of the fracture surface was carried out using an optical microscope at magnifications of 100× and 500×. The microstructures of samples 1 and 2 were similar, showing banding parallel to the longitudinal axis of the bolt (Fig. 5a) and tempered martensite (Fig. 5b).

Based on microstructural examination using a measuring reticle, the thickness of the hot-dip galvanized layer was determined to be 82-155 µm. For reference, EN ISO 10684 specifies a minimum local coating thickness of 40 µm and a minimum batch-average coating thickness of 50 µm [15]. The galvanized layer was partially damaged (Fig. 6a), and cracks were also observed in the coating (Fig. 6b).

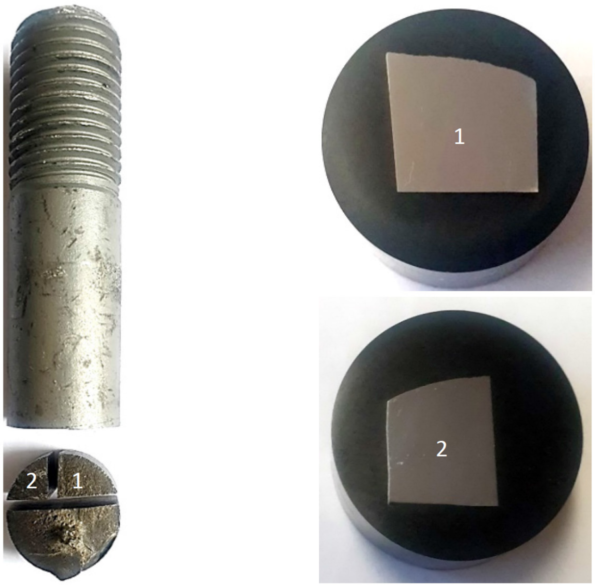

a) b)

Fig. 4 Sampling for microscopic analysis: (a) cutting a part of the bolt shank with a fracture surface; (b) mounted metallographic samples 1 and 2

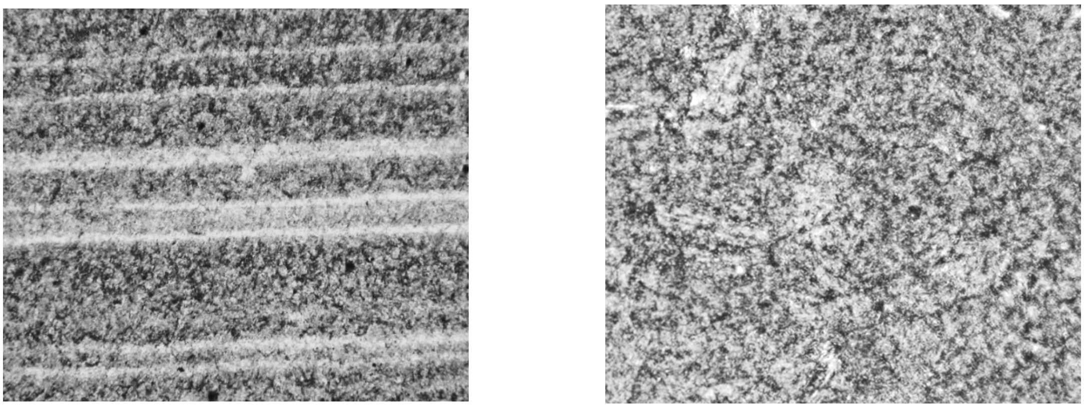

a) b)

Fig. 5 Photographs of the cross-section of the fracture surface of tested samples 1 and 2: (a) banded microstructure (magnification 100×); (b) tempered martensite (magnification 500×)

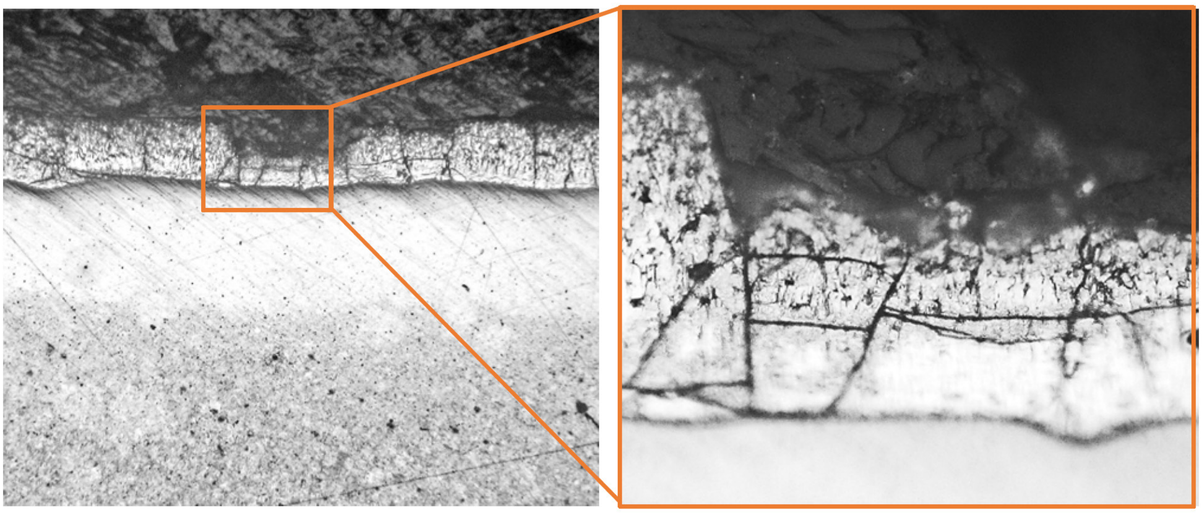

a) b)

Fig. 6 Photographs of the cross-section of the zinc layer: (a) damage to the zinc layer (magnification 100×); (b) cracks in the galvanized coating (magnification 500×)

3.4 Hardness measurements

Vickers hardness testing [16] was performed on mounted metallographic samples in the fracture zone, i.e., below the fracture surface. A semi-automatic HENRI HAUSER-BIENE 249a optical hardness tester was used with a test force of 9.807 N (HV1). Fig. 7 shows the locations of the measuring points and the measured hardness values on mounted metallographic samples 1 and 2 (see Fig. 4).

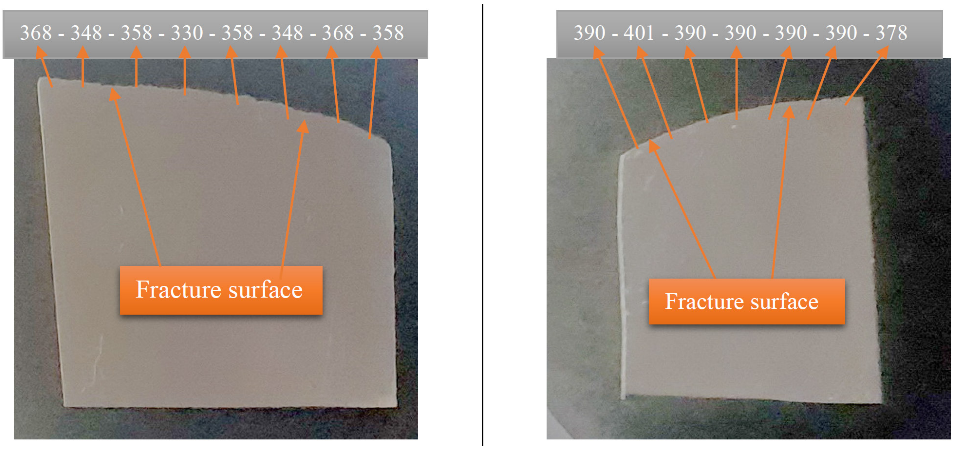

a) b)

Fig. 7 Location of measurement points and measured hardness values (HV1) on mounted metallographic samples 1 and 2: (a) sample 1; (b) sample 2

4. Discussion

According to the client, the high-strength class 10.9 bolt failed a few days after installation. The fracture morphology in Fig. 3 indicates that an initial crack formed at the head-to-shank junction and propagated rapidly to final failure. Considering the short time to failure, the high-strength 42CrMo4 steel, and the sequence of heat treatment and hot-dip galvanizing, hydrogen embrittlement (HE) is the most likely failure mechanism [17, 18]. Because the bolt was installed in a statically loaded structure for only a short period, fatigue is unlikely to have been the dominant failure mechanism.

The measured coating thickness of 82-155 μm is above the minimum local coating thickness specified in EN ISO 10684 [15]. However, coating thickness alone does not establish galvanizing immersion time or hydrogen uptake; therefore, its role in the present failure cannot be determined from the available data. Cracks and microcracks in the hot-dip galvanized layer may act as local stress concentrators. In the presence of hydrogen and sustained tensile stress, such defects may contribute to susceptibility to hydrogen-assisted brittle fracture [19, 20].

Apart from carbon, which was measured below the nominal range, the chemical composition of the tested steel was within the prescribed values for grade 42CrMo4. The bolt was quenched and tempered, and its microstructure consists of tempered martensite. Banding parallel to the bolt axis was also observed; however, it was not considered the primary cause of the fracture.

Several subsurface hardness values exceeded 350 HV1, with a maximum measured value of 401 HV1 (Fig. 7). Such elevated hardness increases the susceptibility of high-strength steel to hydrogen embrittlement [4]. General guidance also identifies susceptible high-strength material, hydrogen, and sustained mechanical stress as the key conditions for hydrogen embrittlement [21]. The elevated subsurface hardness therefore indicates increased susceptibility to hydrogen embrittlement, consistent with the findings of Zafra *et al.* [22] for quenched and tempered 42CrMo4 steel. Similar delayed-failure behaviour in high-strength hot-dip galvanized bolts was reported by Artola and Aldazabal [23]. Due to equipment and sample-access limitations, high-resolution scanning electron microscopy (SEM) fractography and direct hydrogen measurement could not be performed in this study. This is an important limitation; nevertheless, the combined evidence of elevated subsurface hardness, optical metallography, coating damage, and the short time-to-failure supports hydrogen embrittlement as the most likely mechanism. Future investigations should incorporate SEM characterisation and direct hydrogen measurement to further detail the fracture micromechanisms.

5. Conclusion

The investigated 42CrMo4 steel bolt of property class 10.9 exhibited a tempered martensitic microstructure, local coating damage and cracking, and hardness values of 330-401 HV1. Combined with the short time to failure and static loading, these findings support hydrogen embrittlement as the most likely failure mechanism, although direct hydrogen measurement and SEM fractography were not performed. The results underline the importance of controlling heat treatment, hot-dip galvanizing, and bolt installation procedures to reduce the risk of premature brittle failure.

Acknowledgement

This research is supported by the Ministry of Education, Science and Technological Development of the Republic of Serbia (Contract No. 451-03-33/2026-03/200012).

References

[1] Kovacic, M., Zupanc, A., Zuperl, U., Brezocnik, M. (2024). Reducing scrap in long rolled round steel bars using Genetic Programming after ultrasonic testing, *Advances in Production Engineering & Management*, Vol. 19, No. 4, 435-442, doi: 10.14743/apem2024.4.517.

[2] Sun, Y.Y., Yang, J.H., Zhai, L.Y., Liu, N. (2025). Enhanced product defect forecasting using partitioned attributes and ensemble machine learning, *Advances in Production Engineering & Management*, Vol. 20, No. 2, 157-172, doi: 10.14743/apem2025.2.533.

[3] Boyd, W.K., Hyler, W.S. (1973). Factors affecting environmental performance of high-strength bolts, *Journal of the Structural Division*, Vol. 99, No. 7, 1571-1588, doi: 10.1061/JSDEAG.0003563.

[4] Townsend, H.E. Jr. (1975). Effects of zinc coatings on the stress corrosion cracking and hydrogen embrittlement of low-alloy steel, *Metallurgical Transactions A*, Vol. 6, No. 4, 877-883, doi: 10.1007/BF02672311.

[5] Timmins, P.F. (1997). *Solutions to hydrogen attack in steels*, ASM International, Materials Park, OH, USA.

[6] Levy, E. (1992). Cracking of an alloy steel bolt, in: Esaklul, K.A. (ed.), *Handbook of Case Histories in Failure Analysis*, Vol. 1, ASM International, Materials Park, OH, USA, 303-304, doi: 10.31399/asm.fach.v01.c9001093.

[7] Kerns, G.E., Mighton, C.E. (1992). Fractures of hot dip galvanized steel anchor bolts in chemical plant construction project, in: Esaklul, K.A. (ed.), *Handbook of Case Histories in Failure Analysis*, Vol. 1, ASM International, Materials Park, OH, USA, 328-331, doi: 10.31399/asm.fach.v01.c9001100.

[8] Baggerly, R.G. (1993). Hydrogen-assisted stress cracking of carburized and zinc plated SAE Grade 8 wheel studs, in: Esaklul, K.A. (ed.), *Handbook of Case Histories in Failure Analysis*, Vol. 2, ASM International, Materials Park, OH, USA, 396-400, doi: 10.31399/asm.fach.v02.c9001383.

[9] Dwivedi, S.K., Vishwakarma, M. (2018). Hydrogen embrittlement in different materials: A review, *International Journal of Hydrogen Energy*, Vol. 43, No. 46, 21603-21616, doi: 10.1016/j.ijhydene.2018.09.201.

[10] Carpio, J., Casado, J.A., Álvarez, J.A., Méndez, D., Gutiérrez-Solana, F. (2010). Stress corrosion cracking of structural steels immersed in hot-dip galvanizing baths, *Engineering Failure Analysis*, Vol. 17, No. 1, 19-27, doi: 10.1016/j.engfailanal.2008.11.005.

[11] Acedera, R.A. (2025). Hydrogen safety with hydrogen detection tapes, CAPLINQ, available from: *https://blog.caplinq.com/hydrogen-safety-with-hydrogen-detection-tapes_10381/hydrogen-embrittlement-mechanism*, accessed 28 May 2026.

[12] European Committee for Standardization (2015). EN 14399-4:2015, High-strength structural bolting assemblies for preloading – Part 4: System HV – Hexagon bolt and nut assemblies, CEN, Brussels, Belgium.

[13] European Committee for Standardization (2016). EN 10027-1:2016, Designation systems for steels – Part 1: Steel names, CEN, Brussels, Belgium.

[14] European Committee for Standardization (2006). EN 10083-3:2006/AC:2008, Steels for quenching and tempering – Part 3: Technical delivery conditions for alloy steels, CEN, Brussels, Belgium.

[15] European Committee for Standardization (2004). EN ISO 10684:2004/AC:2009, Fasteners – Hot dip galvanized coatings, CEN, Brussels, Belgium.

[16] European Committee for Standardization (2023). EN ISO 6507-1:2023, Metallic materials – Vickers hardness test – Part 1: Test method, CEN, Brussels, Belgium.

[17] Jones, B., Langill, T. (2012). Hydrogen embrittlement, American Galvanizers Association, available from: *https://galvanizeit.org/knowledgebase/article/hydrogen-embrittlement*, accessed 28 May 2026.

[18] Keba Fastenings (2024). Hydrogen embrittlement: How it affects fasteners and how to prevent it, available from: *https://kebafastenings.com/hydrogen-embrittlement-how-it-affects-fasteners-and-how-to-prevent-it/*, accessed 13 May 2026.

[19] Fastener Europe Magazine (2019). The risk of hydrogen embrittlement of 10.9 and 12.9 grade hot-dip galvanized bolts, available from: *https://www.fastenereurope.com/?h941/what-quality-fasteners-are-subject-to-risk-of-hydrogen-embrittlement*, accessed 17 May 2026.

[20] British Constructional Steelwork Association (2022). Hydrogen embrittlement: Its effect on structural bolting assemblies, available from: *https://steelconstruction.info/images/f/fc/HydrogenEmbrittlementLongVersion_01-08-2022.pdf*, accessed 8 May 2026.
[21] Fastenal Engineering Team (2025). Embrittlement, *The Blue Print*, available from: *https://blueprint.fastenal.com/embrittlement.html*, accessed 15 May 2026.
[22] Zafra, A., Peral, L.B., Belzunce, J., Rodríguez, C. (2019). Effects of hydrogen on the fracture toughness of 42CrMo4 steel quenched and tempered at different temperatures, *International Journal of Pressure Vessels and Piping*, Vol. 171, 34-50, doi: 10.1016/j.ijpvp.2019.01.020.
[23] Artola, G., Aldazabal, J. (2020). Hydrogen assisted fracture of 30MnB5 high strength steel: A case study, *Metals*, Vol. 10, No. 12, Article No. 1613, doi: 10.3390/met10121613.